ORIGINAL PAPER





Studies of FET mobility versus iodine doping of P3HT

Latonya R. Waller¹ · Sam-Shajing Sun^{1,2} · Makhes Behera¹ · Messaoud Bahoura^{1,3}

Received: 22 January 2023 / Accepted: 24 March 2023 / Published online: 11 April 2023 © The Author(s), under exclusive licence to The Materials Research Society 2023

Abstract

Serving as the active layer of organic field effect transistors (OFETs), polymers exhibit inherent advantages such as flexibility, lightweight, cost-effective, and biocompatibility. Doping can dramatically alter and vary the electronic properties of semiconductors, enabling field effect transistor (FET) devices with tunable characteristics. In this study, the charge mobility in a FET with an active layer made of a p-type conjugated polymer poly(3-hexylthiophene-2,5-diyl) (or P3HT) doped with iodine is investigated. Preliminary data shows the FET charge mobility initially increases at low doping concentrations but declines at high doping concentrations. This trend's mechanisms are being analyzed and discussed.

Introduction

Materials known as semiconductors have electrical conductivity levels that fall between those of insulators and conductors. Their significance in the ever expanding and changing technological sector is unmatched, making the money invested in researching them is fully worthwhile. In general, there are two main groups of semiconductor materials: inorganic semiconductors and organic semiconductors. In comparison to the other kinds of semiconductors, inorganic semiconductors have received the most research attention [1–3].

As a result of the technology industry's competitors' increased innovation, the most cutting-edge items have been introduced to the market. Competing technological companies have attempted to materialize and commercialize the organic semiconductor-based technology for use in practical applications since innovation is the key enabling element to stay competitive in the ambitious market [4]. Researchers have long been interested in organic semiconductors (semiconducting polymers) because of their innate characteristics that their inorganic counterparts do not offer.

Innate characteristics of organic semiconductors are that they are flexible, lightweight, cost-effective, and biocompatible [5–7].

The primary goal of this project is to ultimately create an OFET that can produce signals in response to small changes in stimuli and identify optimal doping concentrations. The OFETs used in this experiment were fabricated using a 50 µm channel OFETs. A series of samples of different doping concentrations were prepared, and they were characterized to identify the trend in doping concentration versus mobility. The active layer was doped with concentrations of iodine at 0.25%, 0.5%, 0.75%, 1.0%, 4.0%, and 5.0%. The dopant selection process was meticulously carried out because of the significant impact it had on the devices' overall performance. The goal of the dopant utilized in this work was to modify the electrical conductivity of the organic active layer by encouraging the production of free charge carriers. Given that it would affect the type of charge transfer that occurs at the donor-acceptor interface, the energy offset between the host P3HT's frontier orbitals and those of the dopants was heavily taken into account.

Sam-Shajing Sun ssun@nsu.edu

- Center for Materials Research, Norfolk State University, Norfolk, VA 23504, USA
- Department of Chemistry, Norfolk State University, Norfolk, VA 23504, USA
- Department of Electrical Engineering, Norfolk State University, Norfolk, VA 23504, USA

Experimental details

Device fabrication

The first coating/thin film was octadecyltrichlorosilane (OTS) treatment, which was conducted by immersion in an inert nitrogen atmosphere with a 1 mM concentration of OTS in anhydrous toluene. The devices were submerged for



30 min, retrieved, and washed twice in cyclohexane prior to being dried with pressured nitrogen. To confirm the presence of the monolayer generated by OTS, a water droplet was placed on the dielectric surface of the gate in order to witness the hydrophobic beading. The OTS-passivated surface possesses a lower surface energy than the untreated SiO_2 surface, and the hydrophobicity of the methyl-terminated long-chain alkyl group contributes to reduced water adsorption.

Electron-beam deposition is a type of physical vapor deposition in which a target material is hit with an electron beam generated by a charged tungsten filament in a high-vacuum environment. Atoms of the target material are transformed into the gaseous phase by the electron beam. These atoms then solidify, coating everything in the vacuum chamber (within visual range) with a thin layer of the desired substance. When sufficient vacuum (in the range of 10^{-6} to 10^{-8} mbar) is attained, sublimation begins. The vacuum level affects both the melting point and the mean free path of atoms leaving the surface of sublimated material.

As the level of vacuum increases, the melting temperature of the material falls, and as the chamber pressure decreases, the mean free path increases, as the distance evaporated atoms may travel between collisions increases. Cr and Au have been used to deposit contacts on the surface of the Si wafer in this study, although organic small molecules have also been deposited using the same technique [8, 9], and [10]. The three contacts, source, gate, and drain, were deposited utilizing an enclosure with customized attachment extensions, and a shadow mask. It was built with final dimensions yielding various channel lengths: 30, 40, 50, 60, and 80 µm x 1 mm (as purchased) for typical channel devices.

Given that gold is one of the least reactive elements, it was necessary to apply an adhesive tie layer to prevent gold from escaping off of a SiO2 gate dielectric. Chromium is utilized for this purpose because it passivates easily and has a strong affinity for oxygen. Cr forms bonds with accessible oxy gen on the surface of SiO2 as it is deposited in vacuum. Following chromium deposition, Au is deposited which metallically bonds with Cr to form an alloy. By taking advantage of the bonding between the Cr and SiO2 layers, this enhances the gold layer.

The selection of metals for the source and drain contacts, how they are deposited, and how they are successively processed, can significantly affect how electrons or holes are injected into the organic semiconductor active layer [11–14]. In order for holes to be injected, the metal utilized for the contact must have a low enough work function.

Gold works well for this purpose with P3HT with a Φ_m =5.1 eV which is near that of commonly reported values of the P3HT HOMO (5.0—5.2 eV). Contacts may also be functionalized with the use of a self-assembled monolayer

similar to that of OTS for the gate dielectric surface. A report like this has been made for the use of a passivation layer on gold in conjunction with a pentacene active layer in an OFET [15].

All five of the devices, which had varying channel lengths, were on the same diced wafer for typical low-density OFETs utilizing the mask purchased from Ossila, A 70 nm Au layer was then sublimated at an average rate of 1.5 Å/s—2.7 Å/s by pellet in an electron deposition chamber after a 5 nm chromium adhesion layer at a rate of 0.5 Å/s using a tungsten rod covered with chromium.

The next step was to spin-coat P3HT and iodine-doped P3HT solutions at 1500 rpm for 120 s, followed by a 3000 rpm cycle for 5 s to remove any accumulated solution at the margins of the devices. This was done in a nitrogen environment. In a vacuum oven set to 80 °C, coated devices were then dried for at least 8 h overnight. Undoped P3HT samples were baked in a different vacuum oven than doped samples to avoid accidental vapor doping. A swab dipped in o-dichlorobenzene (o-DCB) was used to clean the device surfaces, enabling the accurate removal of any extra coating.

Doping mechanism

Consider the binary P3HT and iodine composite where heat induces an electron transition from the HOMO of the donor polymer P3HT to the LUMO of the acceptor molecule iodine. This generates a hole in the P3HT HOMO which can transport throughout the polymer chain. The use of iodine to dope P3HT was a widely reported doping method. In o-DCB, a stock solution of 8 mg/mL P3HT was made and swirled all night long for at least 8 h. In order to achieve the final target of 4 mg/mL concentration of P3HT, iodine was weighed into each vial at the proper doping masses. P3HT and iodine were weighed into vials while under the influence of air. Overnight, for at least eight hours, the completed solutions were stirred.

The hue of the vials shifted from brilliant orange (undoped) to brown (doped) as the iodine level rose. In this experiment, 8 mg/mL P3HT stock, Iodine 5% stock, 0.25%, 0.5%, 0.75%, 1.0%, 4.0%, and 5.0% I₂ doped samples were prepared to measure FET mobility. As received, diced wafers had two parallel edges chipped to improve the surface area on which the gate contact would be deposited. After 30 min of washing in an ultrasonic bath with acetone and subsequently isopropanol, the samples were dried in a forced-air stream with blown nitrogen. OTS treatment in nitrogen was carried out using a 1 mM concentration of OTS in anhydrous toluene. After 30 min, the devices were removed and cleaned twice in cyclohexane before being dried with blown nitrogen from a forced air stream. Three contacts, source, gate, and drain, were deposited using a shadow mask, resulting in five channel lengths of 30, 40, 50, 60, and 80 µm with a channel width of 1 mm for each (50 micron µm was tested). Using a chromium-coated tungsten rod, a 5 nm chromium adhesion layer was sublimated via electron beam deposition at a rate of 0.5 Å/s, followed by a 70 nm Au layer at a rate of 1.5–2.7 Å/s through pellet. After the contacts were applied, the devices were exposed to oxygen plasma for 30 s before being moved to an inert environment glovebox.

Characterization

The fully fabricated (50 μ m channel length) OFET devices were tested to characterize their electrical properties and performance. These electrical characterizations were carried out with a Keithley 4200-SCS semiconductor analyzer connected to a Signatone 1160 series probe station. All measurements were conducted at room temperature.

The output electrical characterization was conducted by applying a drain voltage sweep from 0 to -100 V, and by imposing a step gate voltage from +40 V to -40 V at intervals of 20 V. The transfer characteristics of the samples was probed by applying a drain voltage sweep from -0 V to +60 V, at -80 V drain voltage.

Results and discussion

Figure 1 illustrates a completed Bottom-gate/bottom-contact (BGBC) OFET device where P3HT was eliminated from the gate and source/drain contact pads. In comparison to other fabricated devices, this P3HT FET device at a thickness of 21 nm appears best at channel lengths of 50 μ m. To prevent crosstalk or stray current, the devices were separated with a fine razor after being thoroughly cleaned. Classic or standard equation between the conductivity and mobility is shown in Eq. 1, where σ is the conductivity, e is the electron charge, N is the charge carrier concentration, and μ is the intrinsic mobility.

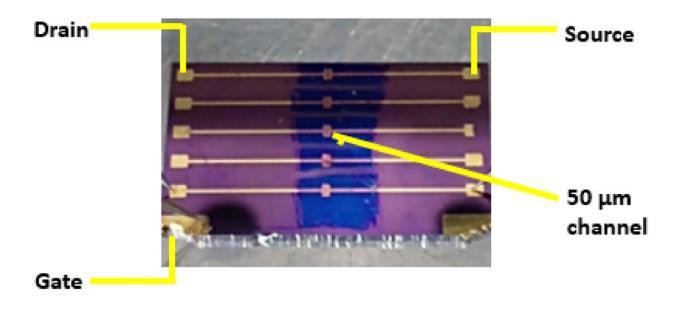


Fig. 1 Shows an illustration of an OFET that has had contacts deposited and the active layer (doped OSC) separated from each of the devices. A single doped OSC spin-coating (purple) over five distinct channel lengths

$$\sigma = eN\mu \tag{1}$$

However, mobility in this equation is also known as the intrinsic mobility, as the conductivity is consisted of both intrinsic mobility and charge density. Equation 2 shows the current FET model used in calculating the mobility in this study.

$$\mu_{SAT} = \frac{2L}{WC_i} \left[\frac{\partial \sqrt{I_D}}{\partial V_G} \right]^2 \tag{2}$$

Output curves

Output curves for this study are shown in Fig. 2.

Transfer curves for this study are shown Fig. 3.

The transfer curves of the OFETs were obtained using a Keithley 4200-SCS semiconductor analyzer. The average data of both forward and reverse multiple sweeps through the voltage range shown generated the transfer curves.

The transfer characteristics measurements are nearly identical to the output current characterization, with the exception that the source-drain current (Ids) is measured by sweeping the drain voltage while holding the drain at a constant value and polarity. The collected data from transfer curves is displayed in the form of Ids vs. Vgs graphs, commonly known as transfer curves.

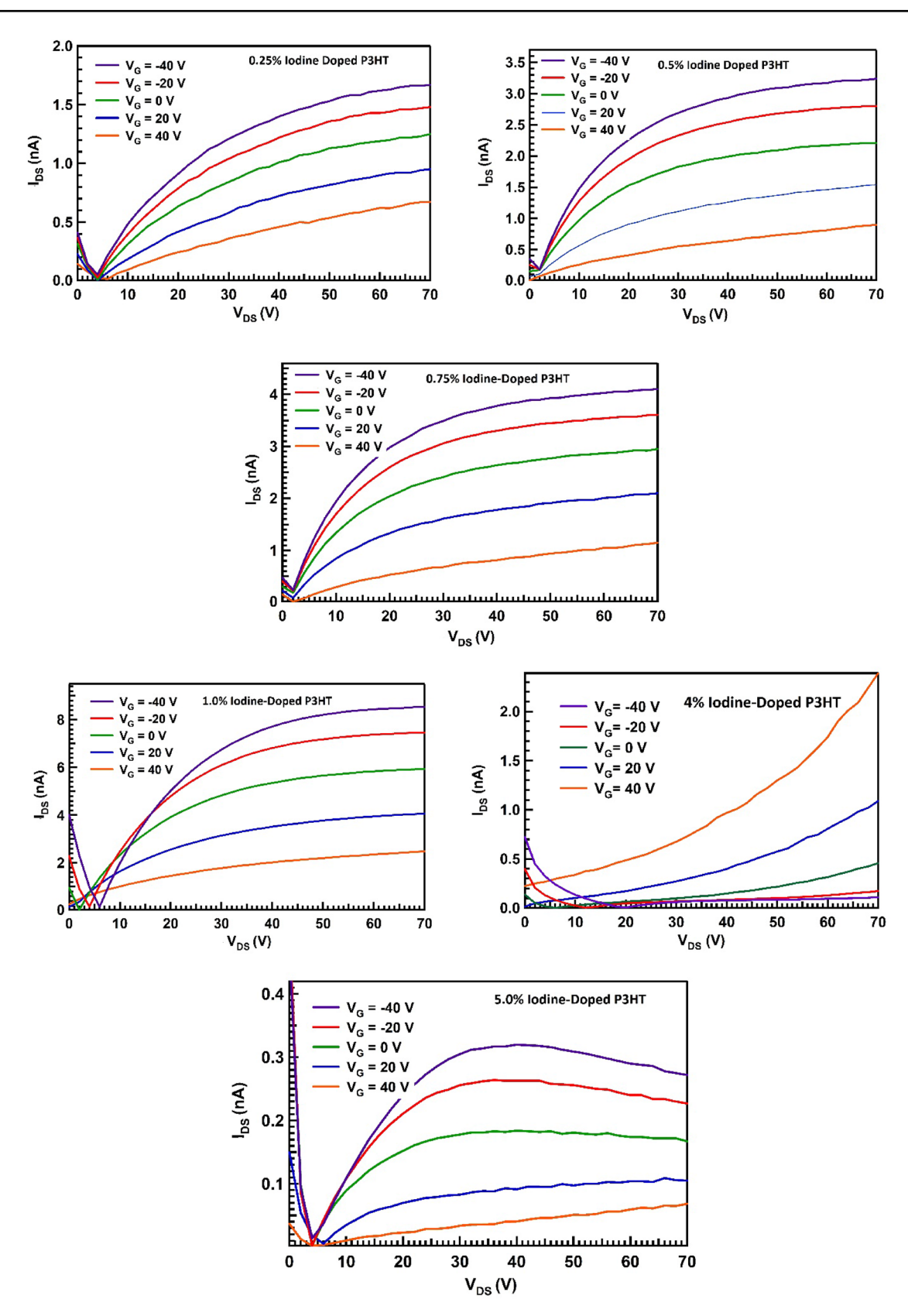
Figure 3 depicts the saturation transfer curves of p-type doped P3HT at iodine doping concentrations of 0.25%, 0.5%, 0.75%, 1.0%, 4.0%, and 5.0%. Carrier mobility was extracted as the key parameter from the FET mobility model based on ' $\rm I_{DS}$ vs $\rm V_{GS}$ ' (transfer) and ' $\rm I_{DS}^{1/2}$ vs $\rm V_{GS}$ ' curves.

The scattering mechanisms in charge transport are accounted for by carrier mobilities, holes, and electrons. As doping concentration increases, intrinsic mobility therefore decreases. This statement implies that homogeneous semiconductor charge mobility is usually saturated. This important source explains why charge mobility declines with rising doping concentration. Basically, charge interactions and/or scattering, are what causes the loss in the intrinsic mobility. The mobility versus iodine dopant concentration graph from this investigation is shown in Fig. 4. After a given concentration, charge scattering causes the FET mobility to decrease.

Since residual charges persist and the initial charge densities are still being consumed, charge density N contributions in the linear region of FETs (either because of iodine doping or Vg) cannot be excluded. In the linear region, residual charges are contributing to conductivity. This is why FET mobility (based on conductivity between source and drain) includes both charge density as well as intrinsic charge mobility. However, in the saturation region, as the

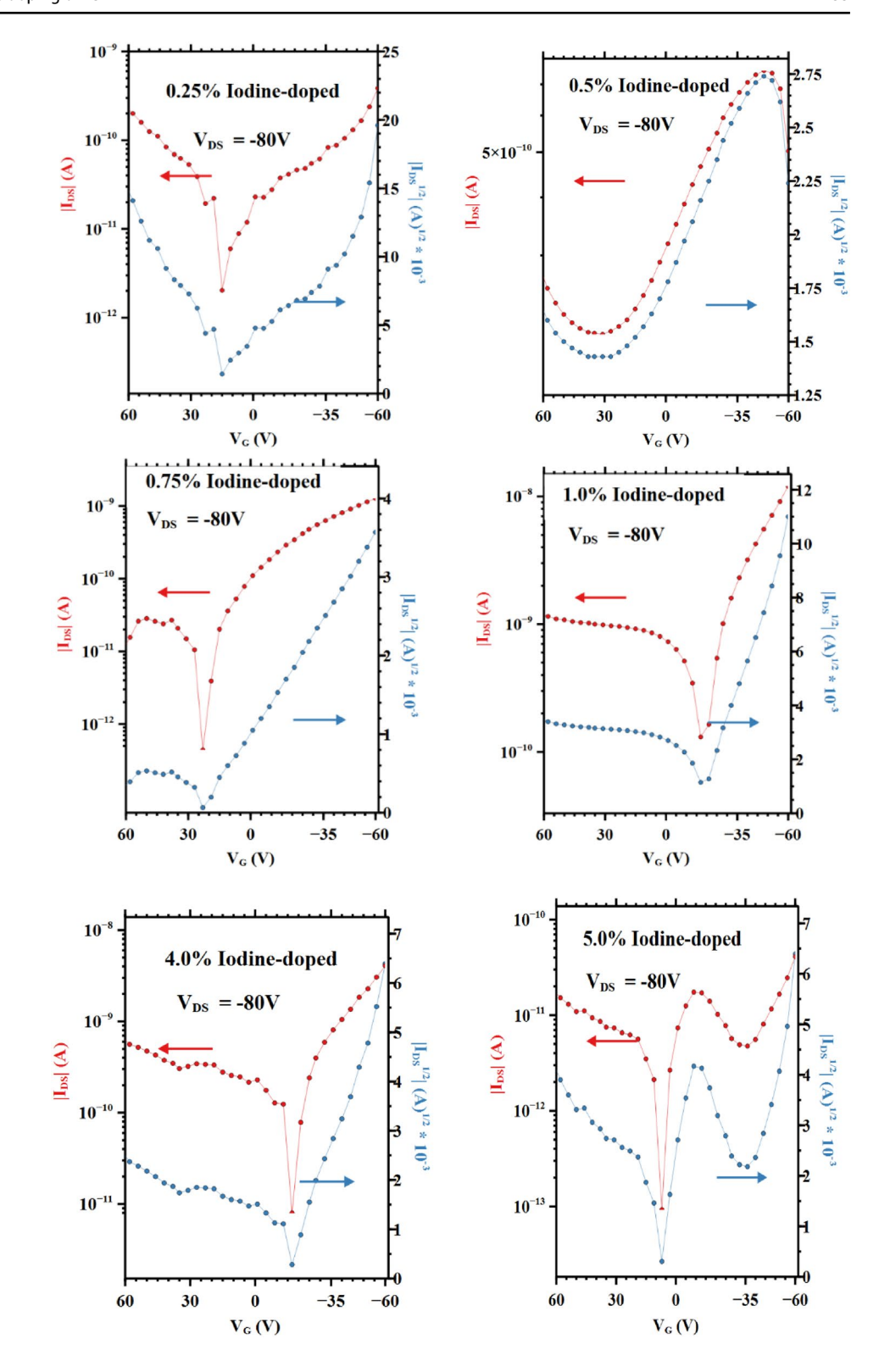


454 L. R. Waller et al.



 $\textbf{Fig. 2} \ \ \text{Output curves for the FET devices at the Iodine doping concentrations of 0.25\%, 0.5\%, 0.75\%, 1.0\%, 4.0\%, and 5.0\% are shown with gate voltages noted on the graph's left side}\\$

Fig. 3 FET device transfer curves of P3HT doped at Iodine doping concentrations of 0.25%, 0.5%, 0.75%, 1.0%, 4.0%, and 5.0%



charge density remains relatively constant, the conductivity (from current measurements) is mostly contributed from intrinsic charge mobility, though doping level still increase average charge density or FET mobility at lower doping levels.

Current FET mobility model is based on the assumption that intrinsic mobility in the saturated region is directly contributing to conductivity. However, in iodine-doped P3HT, at lower iodine doping concentrations, increased charge (mobile holes in P3HT) density contributes to the



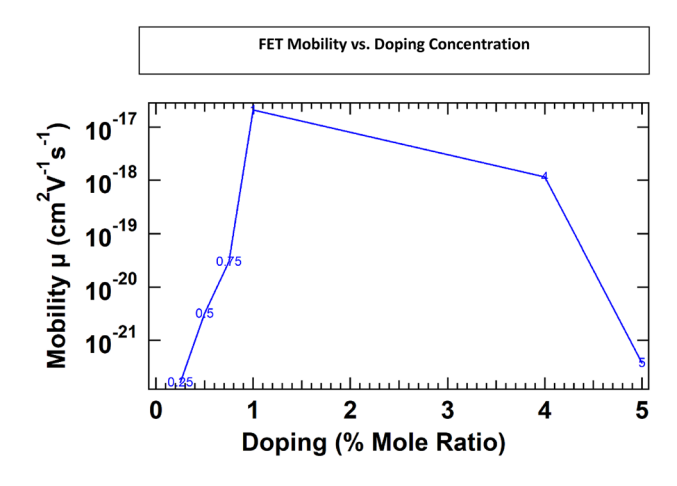


Fig. 4 FET saturated mobility versus iodine doping concentrations

conductivity and therefore FET mobility, this explains why at lower iodine doping levels, FET mobility increases.

Conclusion

This study reveals that P3HT FET hole mobility initially increases at low iodine doping levels due to primarily doping-induced increases in hole density, and that P3HT FET hole mobility decreases at higher iodine doping levels due to primarily electronic charge interactions or lattice scattering causing an intrinsic mobility decrease. Therefore, there exists an ideal iodine doping level or region.

Funding Funding for portions of this project were provided, in part, by a National Science Foundation CREST center grant (award #HRD-1547771). We thank Drs. Joseph W. Norman and Thomas Debesay for certain experimental assistance.

Data availability The datasets generated during and/or analyzed during the current study are available from the corresponding author on reasonable request

Declarations

Conflict of interests On behalf of all authors, the corresponding author states that there is no conflict of interest.

References

 S. Arshavsky-Graham, N. Massad-Ivanir, E. Segal, S. Weiss, Porous silicon-based photonic biosensors: current status and

- emerging applications. Anal. Chem. **91**(1), 441–467 (2018). https://doi.org/10.1021/acs.analchem.8b05028
- O. Bisi, S.U. Campisano, L. Pavesi, Silicon-Based Microphotonics: from Basics to Applications (IOS press, Amsterdam, 1999)
- K.F. Jensen, Silicon-based microchemical systems: characteristics and applications. MRS Bull. 31(2), 101–107 (2006). https://doi. org/10.1557/mrs2006.23
- H.J. Jang et al., Progress of display performances: AR, VR, QLED, OLED, and TFT. J. Inform. Disp. 20(1), 1–8 (2019). https://doi.org/10.1080/15980316.2019.1572662
- J.A. Rivera, A.C. Castillo, M.D.L.L.M. González, Organic Semiconductors (Springer, Cham, 2019), pp.547–573
- K. Liu, B. Ouyang, X. Guo, Y. Guo, Y. Liu, Advances in flexible organic field-effect transistors and their applications for flexible electronics. npj Flex. Electron. (2022). https://doi.org/10.1038/ s41528-022-00133-3
- Y. Sun, Y. Liu, D. Zhu, Advances in organic field-effect transistors. J. Mater. Chem. 15(1), 53 (2005). https://doi.org/10.1039/b411245h
- S. Li, D. Guérin, K. Lmimouni, Improving performance of OFET by tuning occurrence of charge transport based on pentacene interaction with SAM functionalized contacts. Microelectron. Eng. 195, 62–67 (2018). https://doi.org/10.1016/j.mee.2018.04.002
- H.N. Raval, V.R. Rao, OFET Sensors with Poly 3-hexylthiophene and Pentacene as channel materials for ionizing radiation. MRS Proc. 1383, mrsf11-1383 (2012). https://doi.org/10.1557/opl. 2012.184
- H.J. Suk, M.H. Yi, T. Ahn, Thermally crosslinked polyvinyl alcohol (PVA) Layers for the passivation of pentacene thin-film transistors. Mol. Cryst. Liq. Cryst. 578(1), 111–118 (2013). https://doi.org/10.1080/15421406.2013.804783
- L. Bürgi, T.J. Richards, R.H. Friend, H. Sirringhaus, Close look at charge carrier injection in polymer field-effect transistors. J. Appl. Phys. 94(9), 6129–6137 (2003). https://doi.org/10.1063/1.16133 69
- M. Kiguchi, M. Nakayama, T. Shimada, K. Saiki, Electric-field-induced charge injection or exhaustion in organic thin film transistor. Phys Rev B 71(3), 035332 (2005). https://doi.org/10.1103/PhysRevB.71.035332
- D. Natali, L. Fumagalli, M. Sampietro, Modeling of organic thin film transistors: effect of contact resistances. J. Appl. Phys. 101(1), 14501 (2007). https://doi.org/10.1063/1.2402349
- J.W. Park, K.J. Baeg, J. Ghim, S.J. Kang, J.H. Park, D.Y. Kim, Effects of copper oxide/gold electrode as the source-drain electrodes in organic thin-film transistors. Electrochem. Solid-State Lett. 10(11), H340 (2007). https://doi.org/10.1149/1.2774683
- J. Norman, Demonstration of an Electro-Electric and Thermal Electric Dual-Modulation Material and Device, PhD Dissertation, Norfolk State University, Norfolk, Virginia, USA, July 2021

Publisher's Note Springer Nature remains neutral with regard to jurisdictional claims in published maps and institutional affiliations.

Springer Nature or its licensor (e.g. a society or other partner) holds exclusive rights to this article under a publishing agreement with the author(s) or other rightsholder(s); author self-archiving of the accepted manuscript version of this article is solely governed by the terms of such publishing agreement and applicable law.